Supporting Information for

"Measurements of higher alkanes using NO^+ PTR-ToF-MS: significant contributions of higher alkanes to secondary organic aerosols in China"

Chaomin Wang[1,2], Caihong Wu[1,2], Sihang Wang[1,2], Jipeng Qi[1,2], Baolin Wang[3], Zelong Wang[1,2], Weiwei Hu[4], Wei Chen[4], Chenshuo Ye[5], Wenjie Wang[5], Yele Sun[6], Chen Wang[3], Shan Huang[1,2], Wei Song[4], Xinming Wang[4], Suxia Yang[1,2], Shenyang Zhang[1,2], Wanyun Xu[7], Nan Ma[1,2], Zhanyi Zhang[1,2], Bin Jiang[1,2], Hang Su[8], Yafang Cheng[8], Xuemei Wang[1,2], Min Shao[1,2,*], Bin Yuan [1,2,*]

[1] Institute for Environmental and Climate Research, Jinan University, 511443 Guangzhou, China

[2] Guangdong-Hongkong-Macau Joint Laboratory of Collaborative Innovation for Environmental Quality, 511443 Guangzhou, China

[3] School of Environmental Science and Engineering, Qilu University of Technology, 250353 Jinan, China

[4] State Key Laboratory of Organic Geochemistry and Guangdong Key Laboratory of Environmental Protection and Resources Utilization, Guangzhou Institute of Geochemistry, Chinese Academy of Sciences, 510640 Guangzhou, China

[5] State Joint Key Laboratory of Environmental Simulation and Pollution Control, College of Environmental Sciences and Engineering, Peking University, 100871 Beijing, China

[6] State Key Laboratory of Atmospheric Boundary Physics and Atmospheric Chemistry, Institute of Atmospheric Physics, Chinese Academy of Sciences, 100029 Beijing, China

[7] State Key Laboratory of Severe Weather & Key Laboratory for Atmospheric Chemistry of China Meteorology Administration, Chinese Academy of Meteorological Sciences, 100081 Beijing, China

[8]Multiphase Chemistry Department, Max Planck Institute for Chemistry, Mainz 55128, Germany

*Email: Bin Yuan (byuan@jnu.edu.cn) and Min Shao (mshao@pku.edu.cn)

Page S1-S29

Contents of this file

Figure S8. Comparisons of times series of C9-C11 alkanes measured by NO^+ PTR-ToF-MS and GC-MS during PRD campaign.

Figure S9. Comparisons of hourly average diurnal variations of OH exposure calculated from the ratio of benzene and 1,2,4-trimethylbenzene, and isoprene chemistry in PRD and NCP.

Figure S10. (a) Time series of isoprene and monoterpenes in NCP. (b) Diurnal variation of isoprene, monoterpenes and benzene in NCP. (c) Scatter plot of isoprene and monoterpenes versus CO in NCP.

Figure S11. Hourly diurnal variations of concentrations of organic aerosols (OA) in PRD and NCP.

Figure S12. The reported SOA yields as a function of OA concentrations for higher alkanes (C8-C21 alkanes) (a-k) under high-NO_x condition from chamber studies.

Figure S13. The reported SOA yields as a function of OA concentrations for monoaromatics (benzene, toluene, m-xylene, TMB, styrene) (a-e), naphthalenes (naphthalene, methylnaphthalenes, dimethylnaphthalenes) (f-h) and isoprenoids (isoprene and α-pinene) (i-j) under high-NO_x condition from chamber studies.

Figure S14. The time series of SOA produced from higher alkanes (C8-C21 alkanes), monoaromatics (benzene, toluene, C8 aromatics, C9 aromatics and styrene), naphthalenes (naphthalene, methylnaphthalenes, dimethylnaphthalenes) and isoprenoids (isoprene and monoterpenes) as well as the measured SOA concentrations in PRD (a) and NCP (b), respectively.

Figure S15. Scatter plots of total SOA production from higher alkanes (C8-C21 alkanes), monoaromatics (benzene, toluene, C8 aromatics, C9 aromatics and styrene), naphthalenes (naphthalene, methylnaphthalenes, dimethylnaphthalenes) and isoprenoids (isoprene and

monoterpenes) versus measured SOA concentrations during the PRD campaign (a) and NCP campaign (b).

Figure S16. The relative contributions to measured SOA concentrations from higher alkanes (C8-C21 alkanes), monoaromatics (benzene, toluene, C8 aromatics, C9 aromatics and styrene), naphthalenes (naphthalene, methylnaphthalenes, dimethylnaphthalenes) and isoprenoids (isoprene and monoterpenes) in PRD (a) and NCP (b).

Figure S17. Hourly diurnal variations of SOA mass yield of *n*-C15 alkane, Benzene, Naphthalene and α-Pinene in PRD (a) and NCP (b).

Figure S18. The mean SOA production rates of higher alkanes (C8-C20 alkanes), monoaromatics (benzene, toluene, C8-aromatics, C9-aromatics and styrene), naphthalenes (naphthalene, methylnaphthalenes, dimethylnaphthalenes) and isoprenoids (isoprene and monoterpenes) and their hourly diurnal variations in PRD and NCP, respectively.

Figure S19. Hourly diurnal variations of OH concentrations in PRD and NCP, respectively.

1. Description of sampling sites

The sampling site of Guangzhou Campaign (23.13º N, 113.26 º E) was on the top of a nine-story building (25 m above ground level) at Guangzhou Institute of Geochemistry, Chinese Academy of Sciences. This site is a typical urban site surrounded by residential areas, campus and urban transport arteries with a strong influence of vehicle emissions. Field measurements of site Baoding (38.85º N, 115.48º E) were performed on the top of a sea container (3.5 m above ground level) located at a Meteorological Auto-Monitoring Station in the rural area of North China Plain. This rural site was surrounded by farmlands and villages, with several national roads and railways nearby, where air masses are influenced from local emissions and regional transport.

2. Estimation of SOA production from individual precursors

It is assumed that VOCs are removed from the atmosphere mainly by reaction with OH radical(Atkinson and Arey, 2003), then the VOCs are assumed to follow a pseudo first-order kinetic reaction, such as

$$-\frac{d[VOC_i]}{dt} = k_{VOC_i}[VOC_i][OH] \quad (1)$$

where$[VOC_i]$ is the concentration of a given VOC (μg m^{-3}), [OH] is the concentration of OH radical (molecule cm-^{3}), k_{VOC_i} is the rate constant of VOC_i with the OH radical (cm^{3} molecule^{-1} s^{-1}). The initial concentration of a given VOC, $[VOC_i]_{t=0}$ can be retrieved from Eq. (1) as follows:

$$[VOC_i]_{t=0} = [VOC_i]_t \times (e^{k_{VOC_i} \times [OH] \times \Delta t}) \quad (2)$$

$[VOC_i]_t$ is the VOC_i concentration measured at time *t* (μg m^{-3}), The OH exposure, $[OH] \times \Delta t$ (molecules cm^{-3} s), is estimated by the ratio of 1,2,4-trimethylbenzene to benzene(de Gouw et al., 2017;Hayes et al., 2013) for anthropogenic VOCs and by isoprene chemistry method

for biogenic VOCs, respectively(Carlton et al., 2009) (Figure S8). Then consumed concentration of a given VOC, $\Delta[VOC_i]$, can be estimated as follows:

$$\Delta[VOC_i] = [VOC_i]_{t=0} - [VOC_i]_t \quad (3)$$

$$\Delta[VOC_i] = [VOC_i]_t \times (e^{k_{VOC_i} \times ([OH] \times \Delta t)} - 1) \quad (4)$$

Then for a given VOC, the SOA production (μg m^{-3}) at time t, $[SOA_i]_t$, can be estimated using the consumed concentration multiply the SOA yield, $Yield_i$, as follows:

$$[SOA_i]_t = [VOC_i]_t \times (e^{k_{VOC_i} \times ([OH] \times \Delta t)} - 1) \times Yield_i \quad (5)$$

3. Estimation of contributions of individual precursors to SOA production

We calculated the relative contribution of each compound to the total SOA concentration at time *t* by

$$[Fraction_i]_t = \frac{[SOA_i]_t}{[SOA_{measured}]_t} \times 100 \quad (6)$$

where $[Fraction_i]_t$ (%) is the relative contribution of a given compound VOC_i to the measured SOA total concentration, $[SOA_i]_t$ is the SOA production of VOC_i at time t by the equation (6), $[SOA_{measured}]_t$ is the SOA concentration at time *t*, which is determined by positive matrix factorization (PMF) analysis of organic aerosol measured by aerosol mass spectrometry (μg m^{-3}).

4. Estimation of SOA production rate from individual precursors

Here we calculated the SOA production rate associated with OH radicals for each SOA precursors based on the diurnal variation of each species. Here, only the oxidation of OH radicals is considered(Atkinson and Arey, 2003). The SOA production rate represents the instant SOA production amount by oxidation reaction with atmospheric OH radical at a certain time for a specific precursor, which can be characterized as follows:

$$[SOA_i]_t = [VOC_i]_t \times [OH]_t \times k_{VOC_i} \times Yield_i, \quad (7)$$

where for a given specific compound VOC_i, $[SOA_i]_t$ is the instant SOA production rate for the species (μg m^{-3} s^{-1}), $[VOC_i]_t$ is the concentration measured at time t (μg m^{-3}), $[OH]_t$ is the OH concentration at time t (molecules cm^{-3}), k_{VOC_i} is the rate constant of VOC_i with the OH radical (cm^3 $molecule^{-1}$ s^{-1}) and $Yield_i$ is the SOA yield.

Based on equation (7), SOA instant production for higher alkanes (C8-C20), monoaromatics (benzene, toluene, C8 aromaics, C9 aromaics), naphthalenes (naphthalene, methylnaphthalenes, dimethylnaphthalenes) and isoprenoids (isoprene, monoterpenes) were calculated. The OH reaction rate constant of each compound was taken literature(Atkinson, 2003). SOA yield data used here for alkanes (Lim and Ziemann, 2009;Presto et al., 2010a;Loza et al., 2014;Lamkaddam et al., 2017a), monoaromatics(Li et al., 2016;Tajuelo et al., 2019;Ng et al., 2007), naphthalenes (Chan et al., 2009) and isoprenoids (Ahlberg et al., 2017;Carlton et al., 2009;Edney et al., 2005;Kleindienst et al., 2006;Pandis et al., 1991) were summarized from reported values in the literature, with the consideration on the influence of organic aerosol concentration (Figure S11) to SOA yield (Figure S12-13). OH concentrations are derived from an observation-constrained box model utilizing MCM v3.3.1 as the chemical mechanisms(Wolfe et al., 2016).

As shown in Figure S18, the total mean SOA production rate of higher alkanes (C8-C20) is much higher compared to other VOCs classes, ~1.9 times of monoaromatics, ~7.8 times of naphthalenes and ~2.4 times of isoprenoids at the urban site in PRD. At the rural site in NCP, the total mean SOA production rate of higher alkanes (C8-C20) is comparable to monoaromatics and slightly higher than that of naphthalenes and isoprenoids. Strong diurnal variations are observed in both sites. In comparison with the rural site in NCP, SOA production rates of VOCs are much higher at the urban cite in PRD. This is mainly due to

the higher OH concentrations (Figure S19) by strong solar radiation under high humidity conditions in PRD during autumn, compared to dry and cold environment during the measurements in NCP

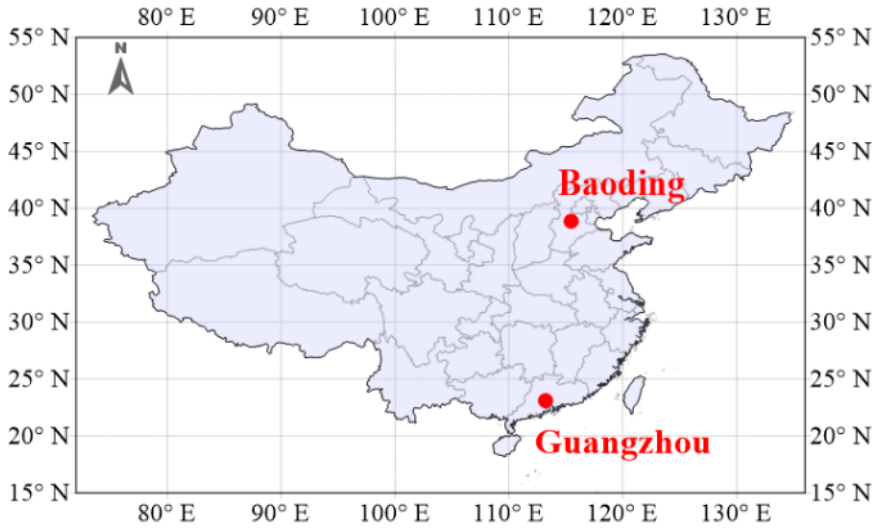

Figure S1. Sampling site locations of Guangzhou Campaign in PRD and Baoding Campaign in NCP of China.

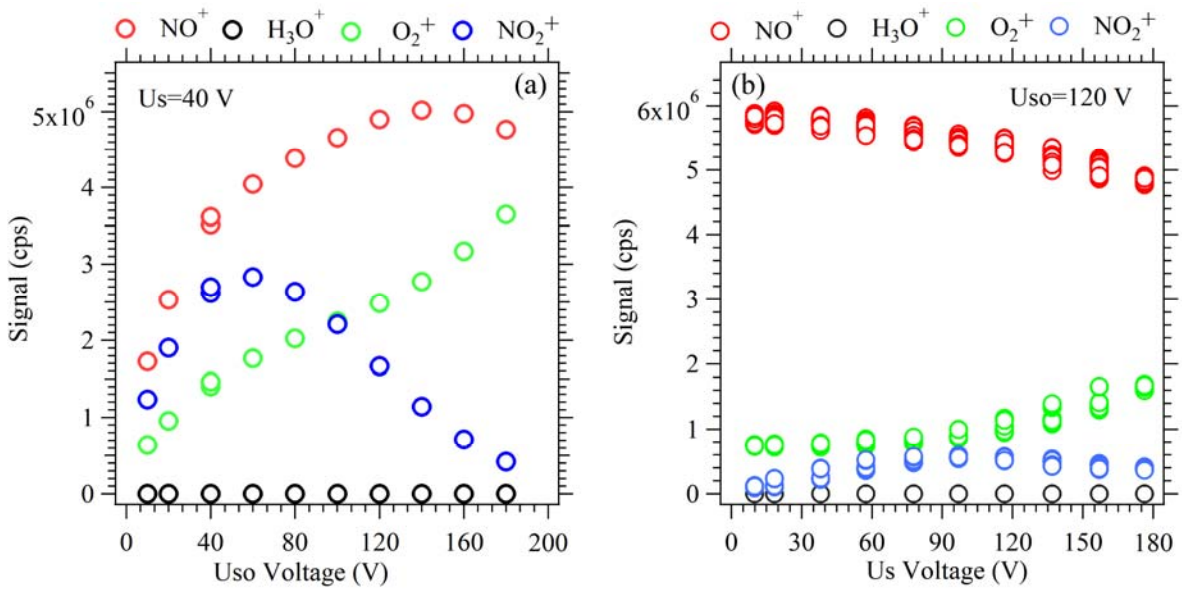

Figure S2. Dependence of NO^+, H_3O^+, O_2^+ and NO_2^+ ions on ion source voltages for NO^+ PTR-ToF-MS.

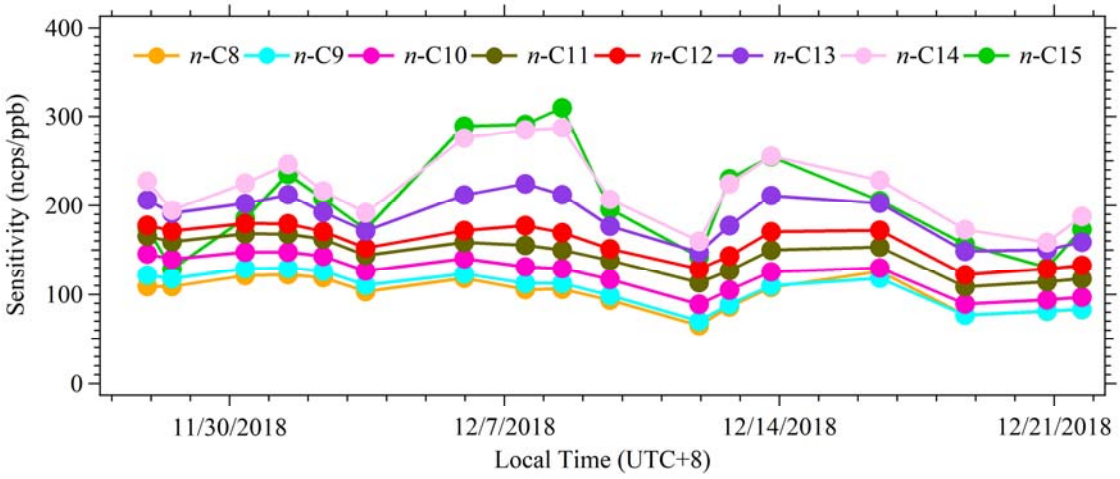

Figure S3. Calibration factors of C8-C15 *n*-alkanes under dry conditions (RH<1%) during the two field campaigns.

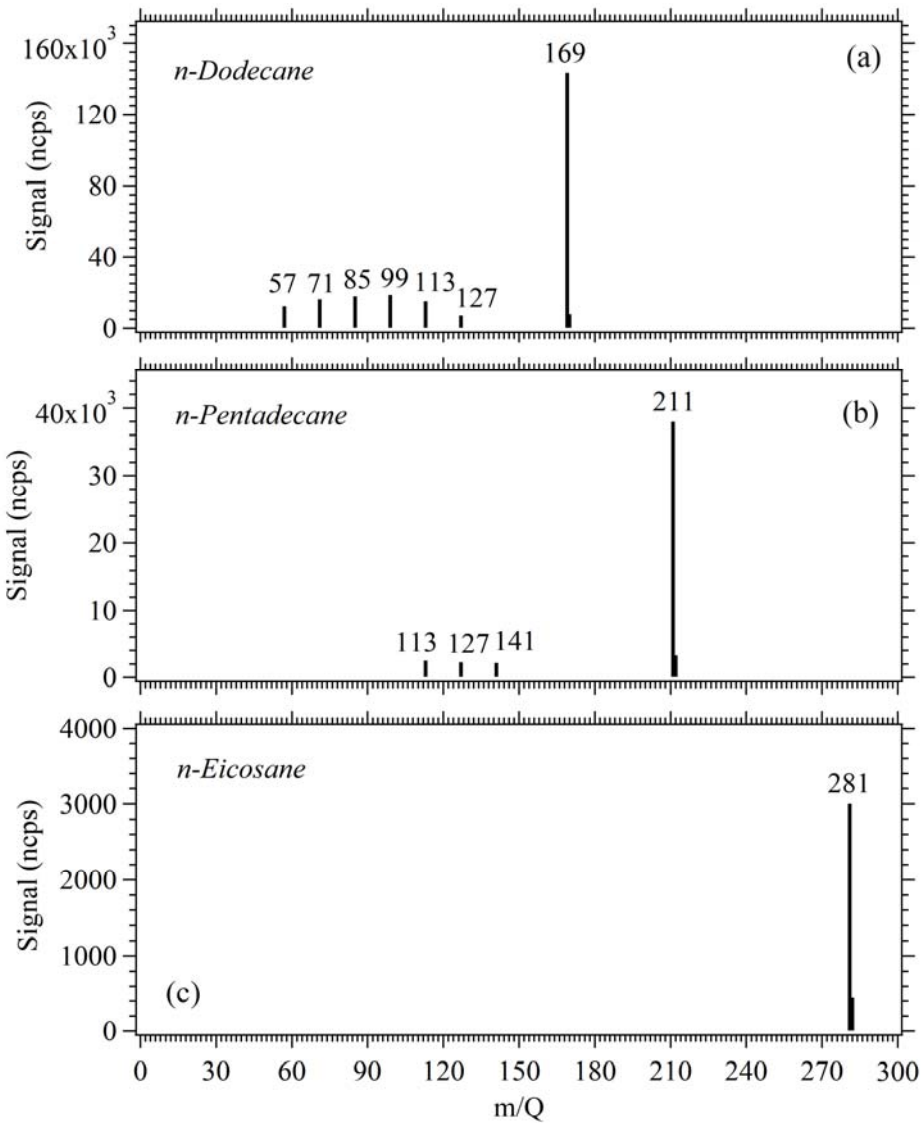

Figure S4. Mass spectra of *n*-Dodecane **(a)**, *n*-Pentadecane **(b)** and *n*-Eicosane **(c)** with NO^+ PTR-ToF-MS.

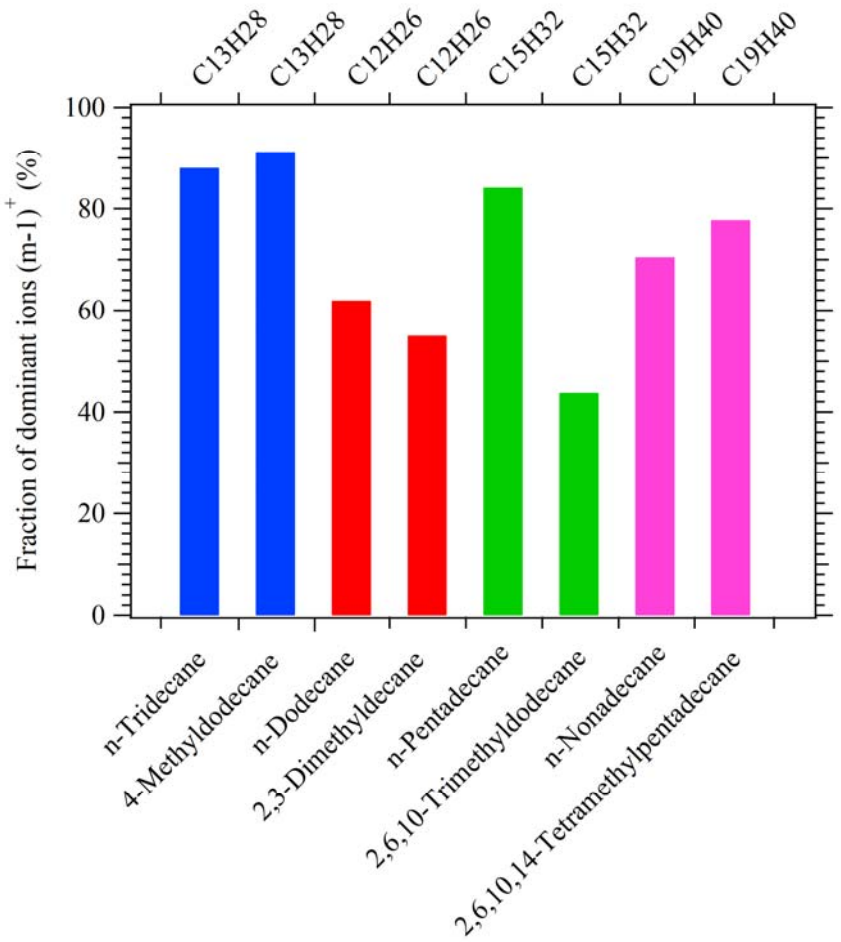

Figure S5. Fraction of product ions $(m\text{-}1)^+$ in the mass spectra of *n*-alkanes and their isomers with different number of substituted methyl groups in NO^+ PTR-ToF-MS.

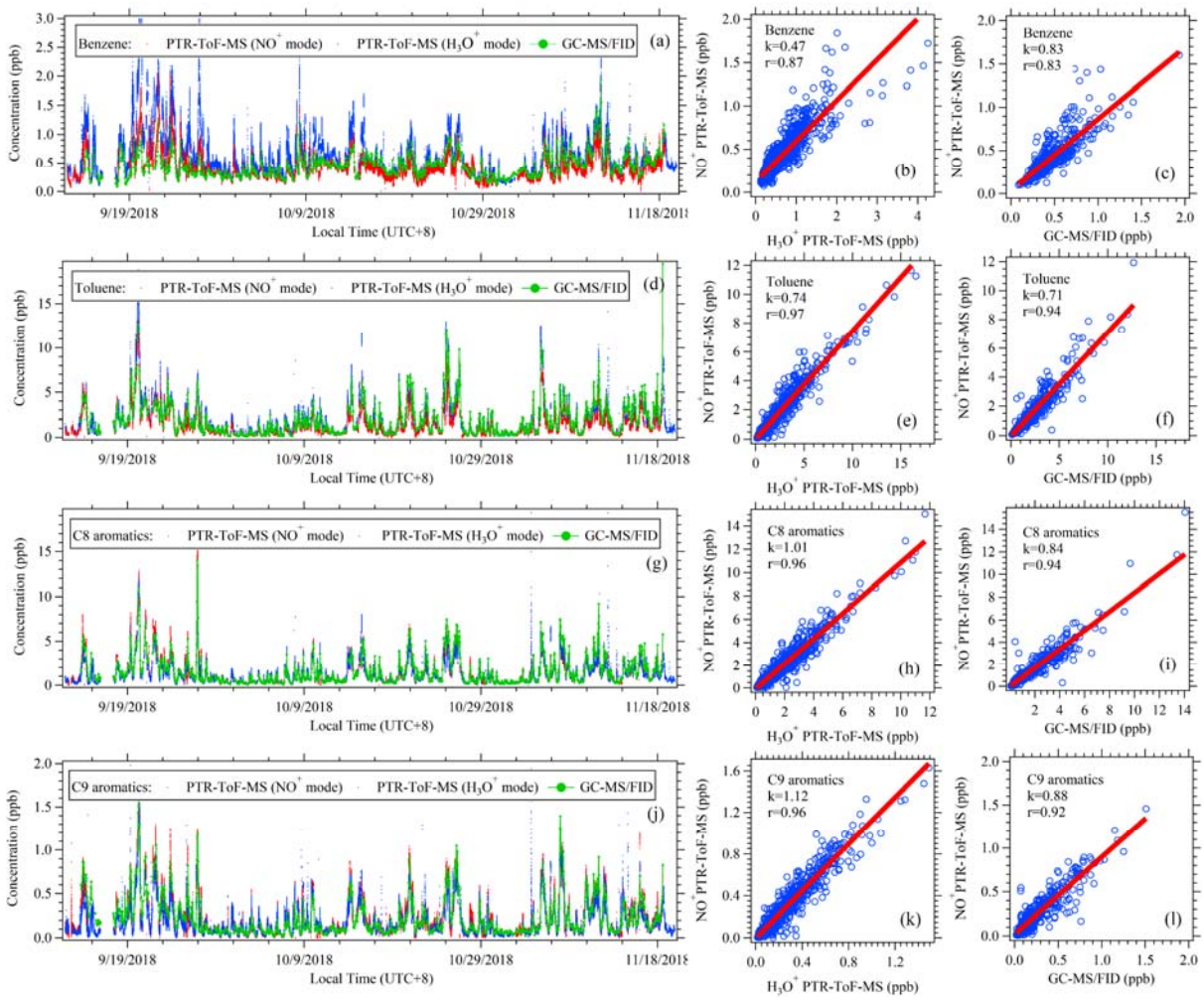

Figure S6. Comparisons of benzene, toluene, C8 aromatics and C9 aromatics measured by NO^+ PTR-ToF-MS (red dots), H_3O^+ PTR-ToF-MS (blue dots) and GC-MS/FID (green lines and dots) during the PRD campaign.

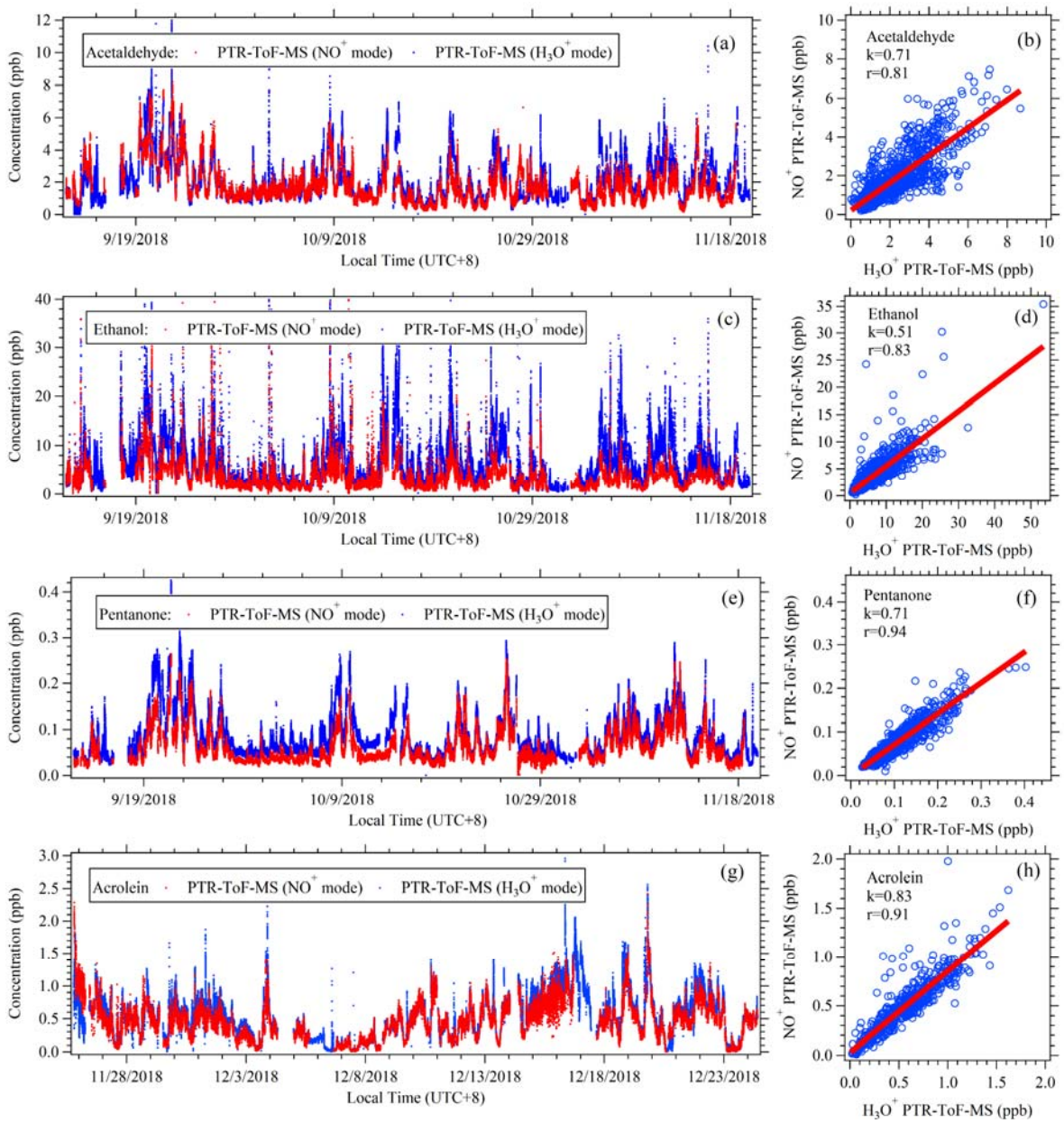

Figure S7. Comparisons of acetaldehyde, pentanone, ethanol and acrolein measured by NO^+ PTR-ToF-MS (red dots) and H_3O^+ PTR-ToF-MS (blue dots) during the PRD and NCP campaigns.

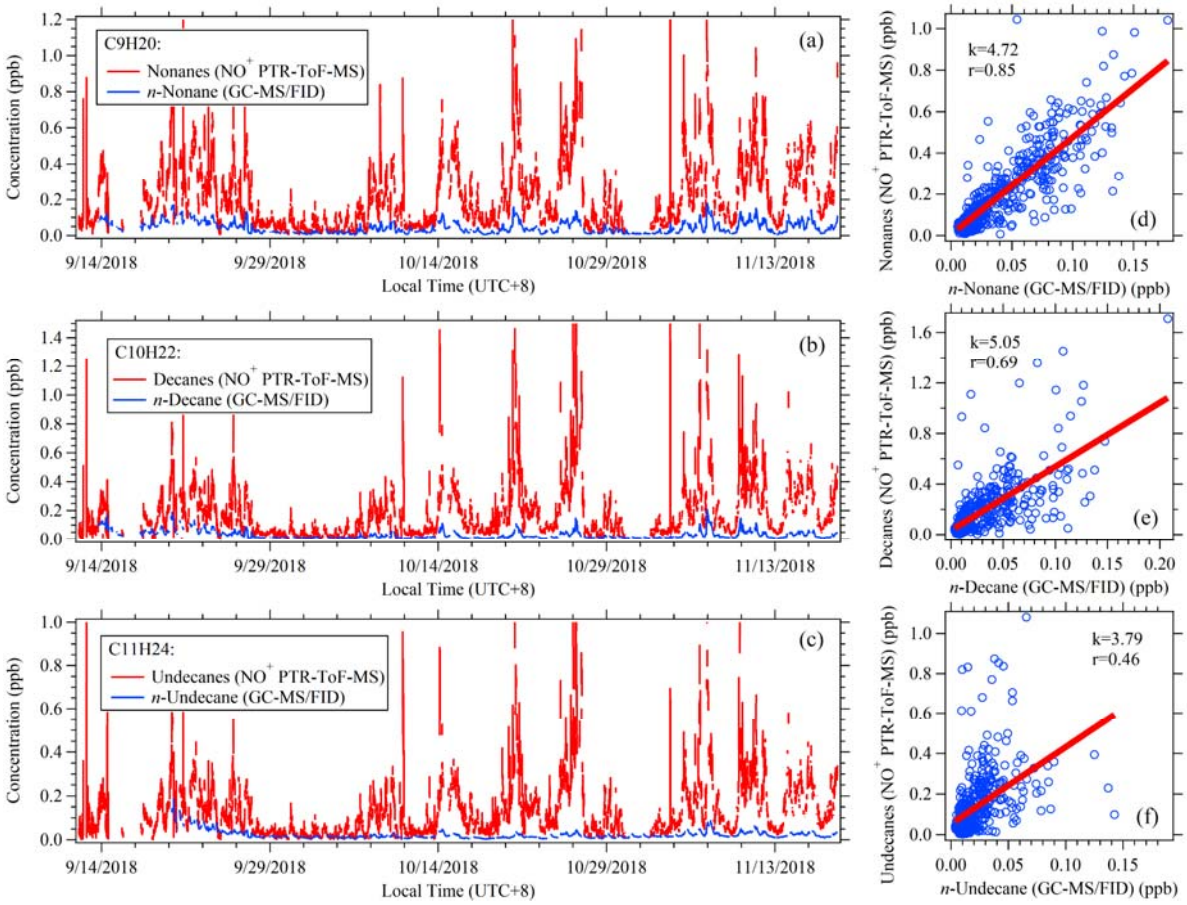

Figure S8. Comparisons of C9-C11 alkanes measured by NO^+ PTR-ToF-MS and GC-MS/FID during PRD campaign.

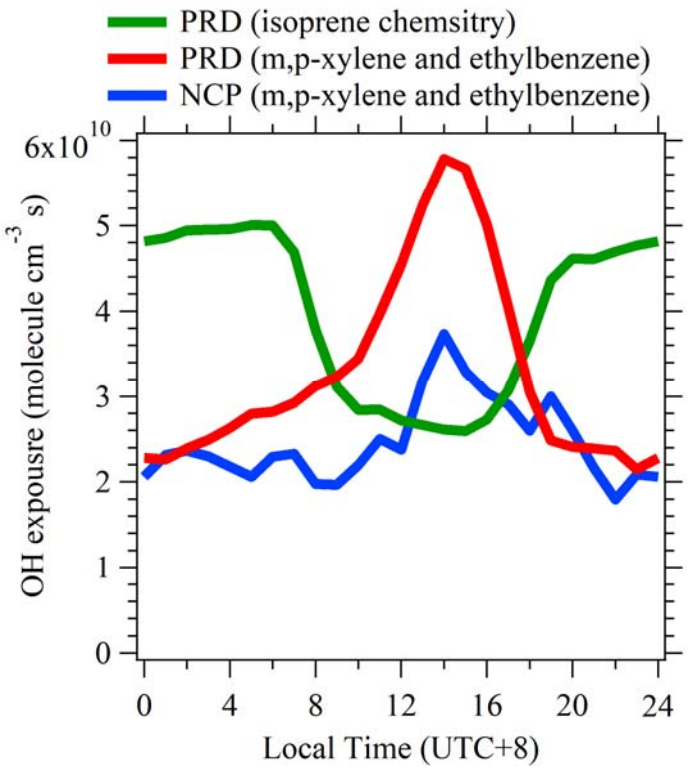

Figure S9. Comparisons of average diurnal variations of OH exposure calculated from the ratio of m+p-xylene and ethylbenzene for anthropogenic compounds in PRD and NCP and isoprene chemistry in PRD for biogenic compounds.

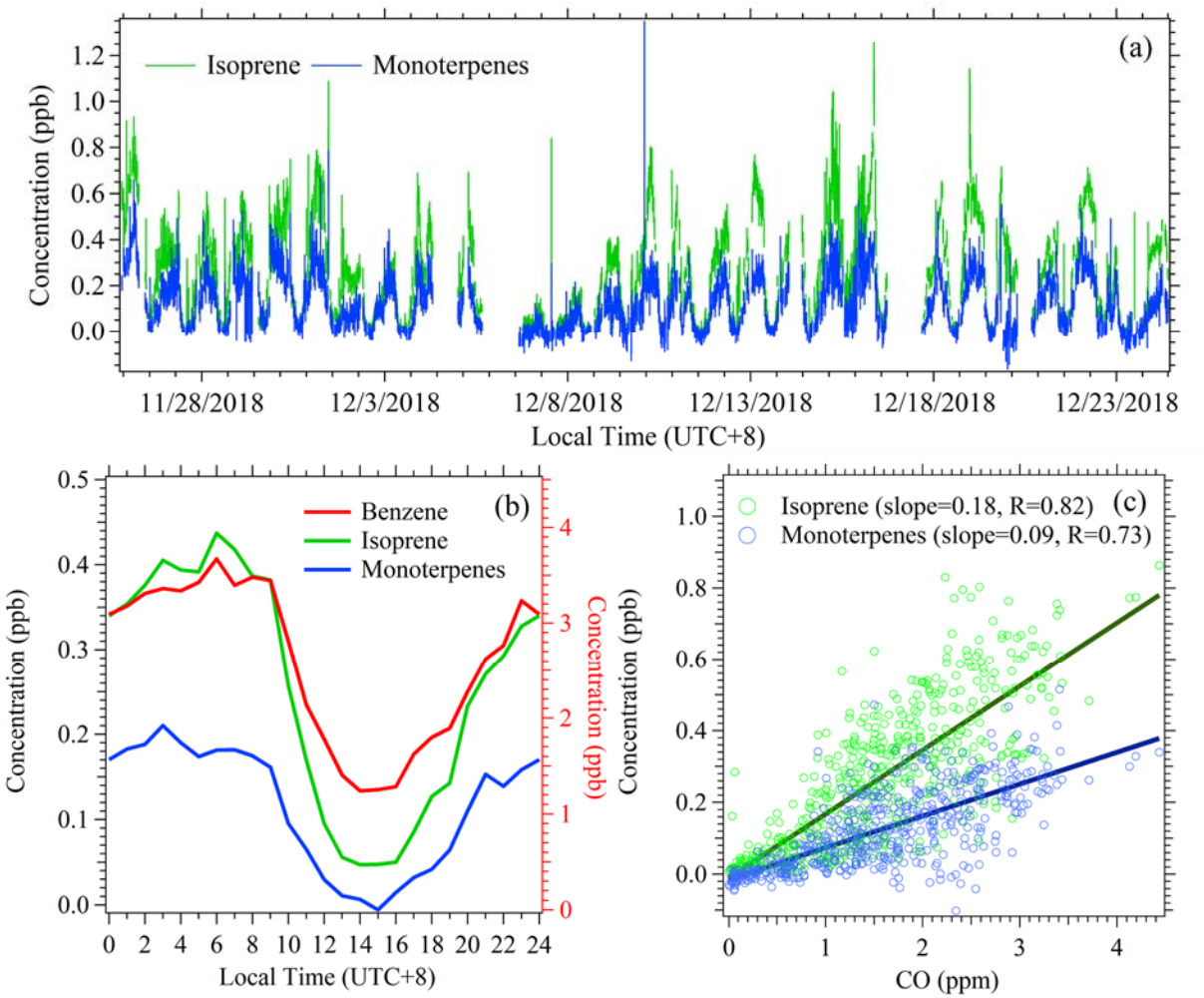

Figure S10. **(a)** Time series of isoprene and monoterpenes in NCP. **(b)** Diurnal variation of isoprene, monoterpenes and benzene in NCP. **(c)** Scatter plot of isoprene and monoterpenes versus CO in NCP.

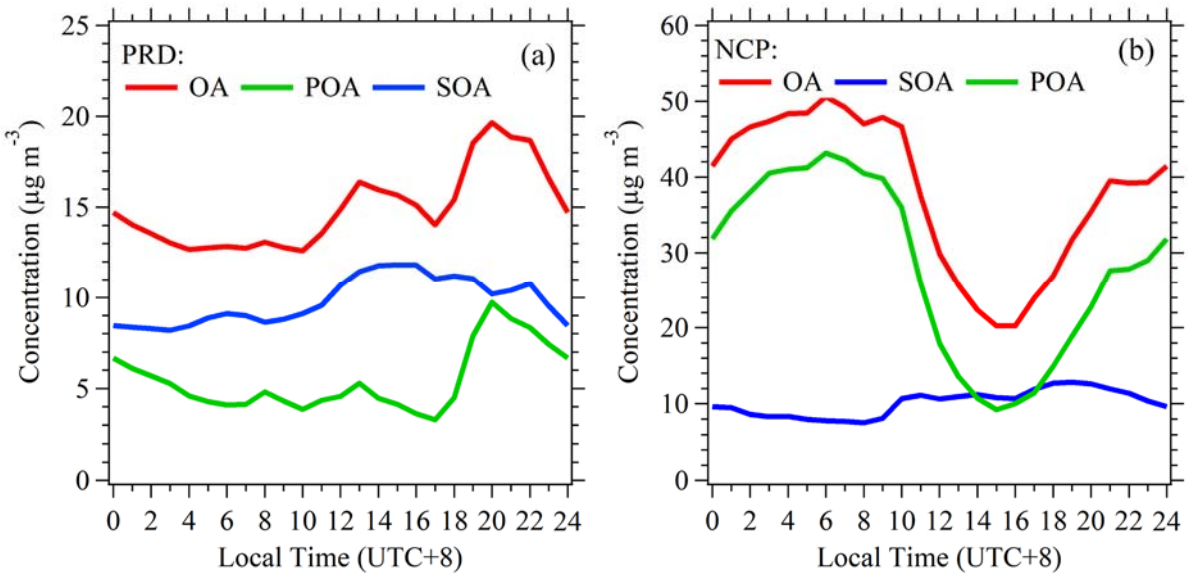

Figure S11. Diurnal variations of concentrations of organic aerosols (OA), secondary organic aerosols (SOA) and primary organic aerosols (POA) in PRD **(a)** and NCP **(b)**. POA and SOA were determined by positive matrix factorization (PMF) analysis of OA measured by AMS.

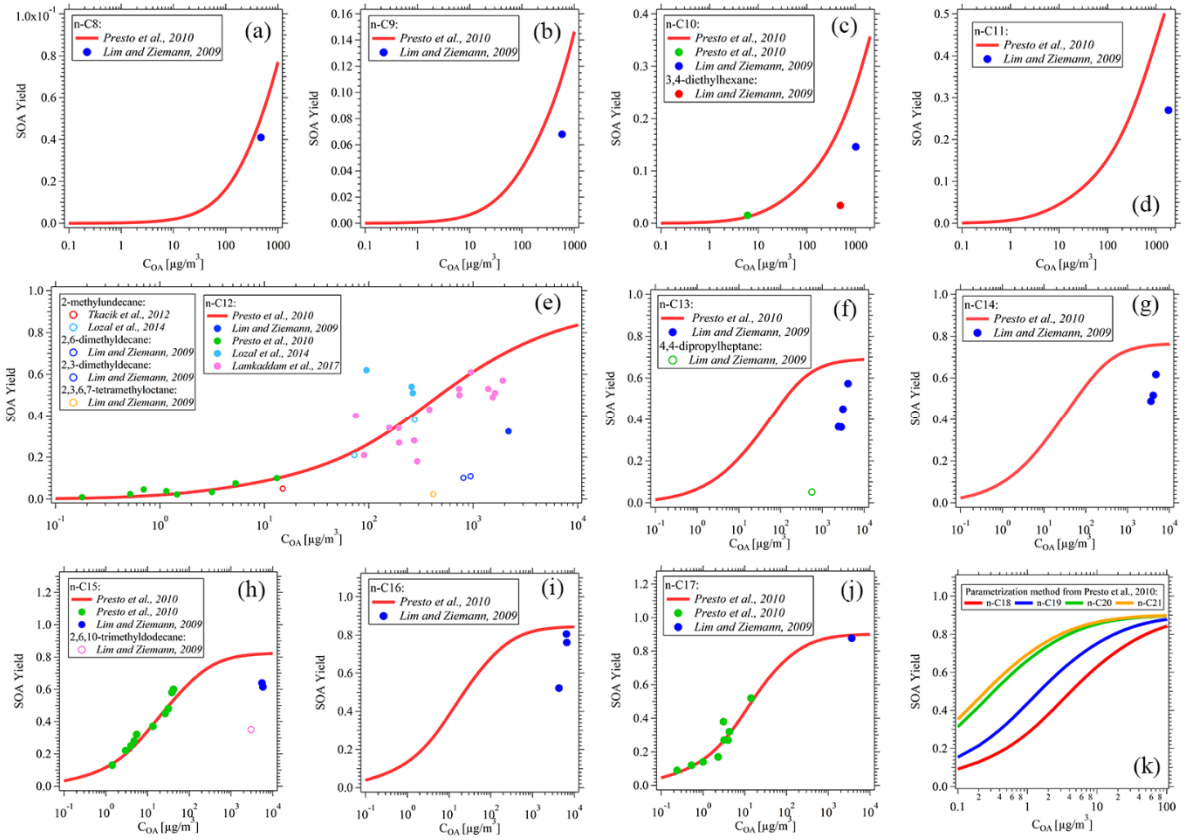

Figure S12. The reported SOA yields as a function of OA concentrations for higher alkanes (C8-C21 alkanes) **(a-k)** under high-NO_x condition from chamber studies(Lim and Ziemann, 2009;Presto et al., 2010b;Tkacik et al., 2012;Loza et al., 2014;Lamkaddam et al., 2017b).

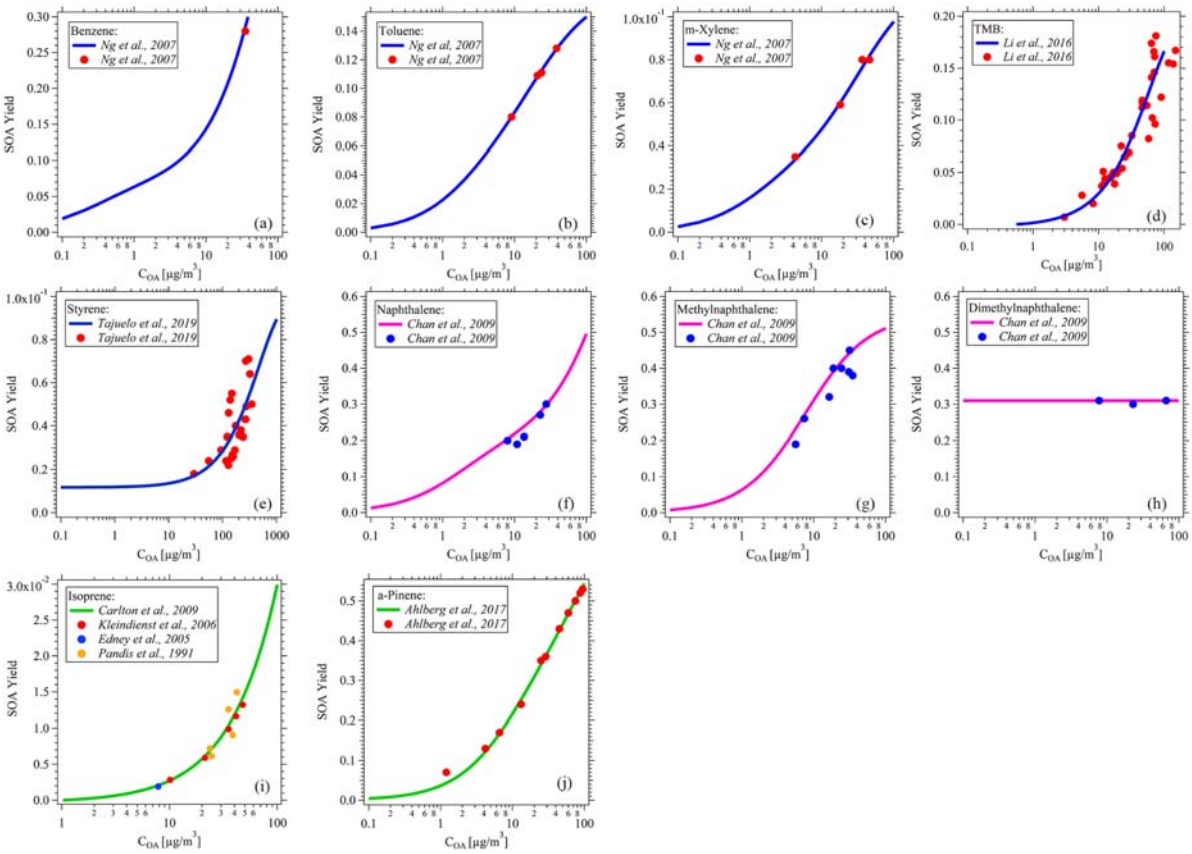

Figure S13. The reported SOA yields as a function of OA concentrations for monoaromatics (benzene, toluene, m-xylene, 1,2,3-TMB/1,2,4-TMB/1,3,5-TMB, styrene)(Ng et al., 2007;Li et al., 2016;Tajuelo et al., 2019) **(a-e)**, naphthalenes (naphthalene, methylnaphthalene, dimethylnaphthalenes)(Chan et al., 2009) **(f-h)** and isoprenoids (isoprene and α-pinene)(Carlton et al., 2009;Edney et al., 2005;Kleindienst et al., 2006;Pandis et al., 1991;Ahlberg et al., 2017) **(i-j)** under high-NO_x condition from chamber studies.

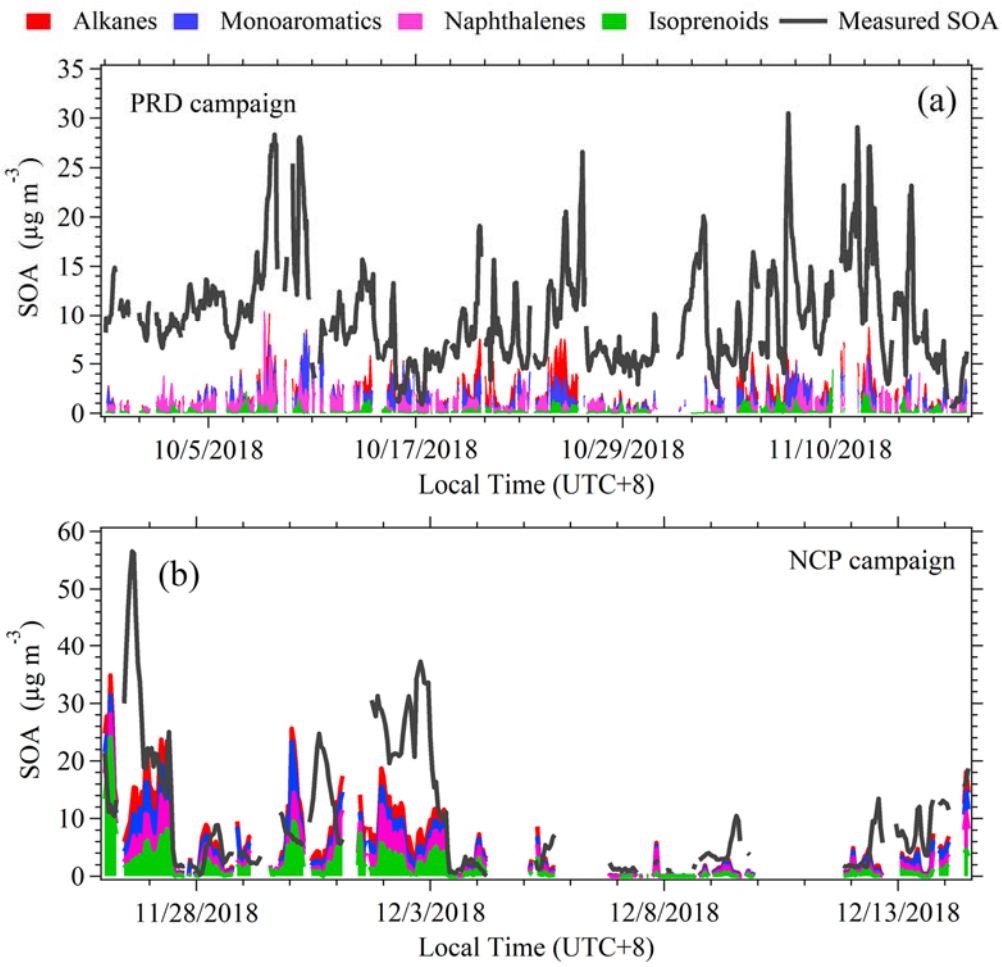

Figure S14. Time series of SOA produced from higher alkanes (C8-C21 alkanes), monoaromatics (benzene, toluene, C8 aromatics, C9 aromatics and styrene), naphthalenes (naphthalene, methylnaphthalenes, dimethylnaphthalenes) and isoprenoids (isoprene and monoterpenes) as well as the measured SOA concentrations in PRD **(a)** and NCP **(b)**, respectively.

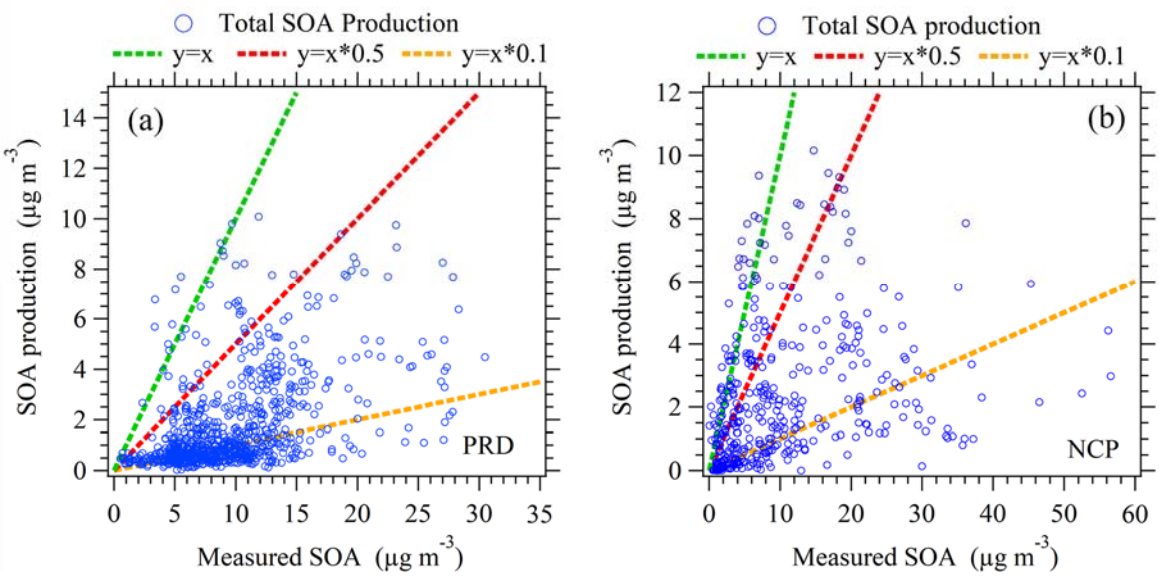

Figure S15. Scatter plots of total SOA production from higher alkanes (C8-C21 alkanes), monoaromatics (benzene, toluene, C8 aromatics, C9 aromatics and styrene), naphthalenes (naphthalene, methylnaphthalenes, dimethylnaphthalenes) and isoprenoids (isoprene and monoterpenes) versus measured SOA concentrations during the PRD campaign **(a)** and NCP campaign **(b)**.

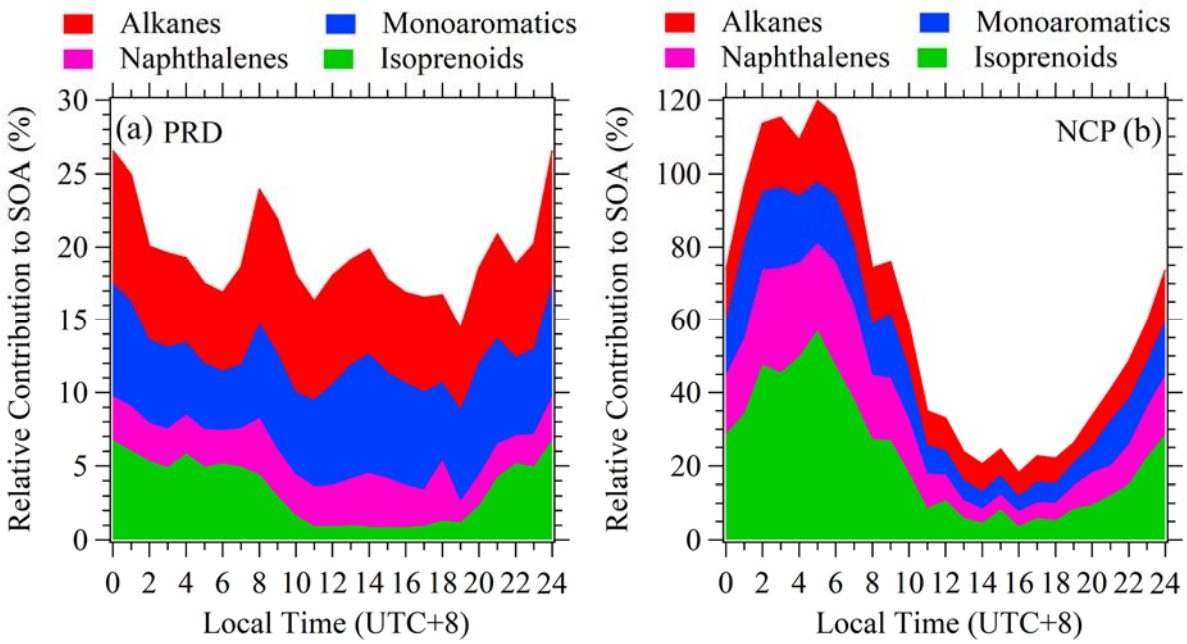

Figure S16. The relative contributions to measured SOA concentrations from higher alkanes (C8-C21 alkanes), monoaromatics (benzene, toluene, C8 aromatics, C9 aromatics and styrene), naphthalenes (naphthalene, methylnaphthalenes, dimethylnaphthalenes) and isoprenoids (isoprene and monoterpenes) in PRD **(a)** and NCP **(b)**.

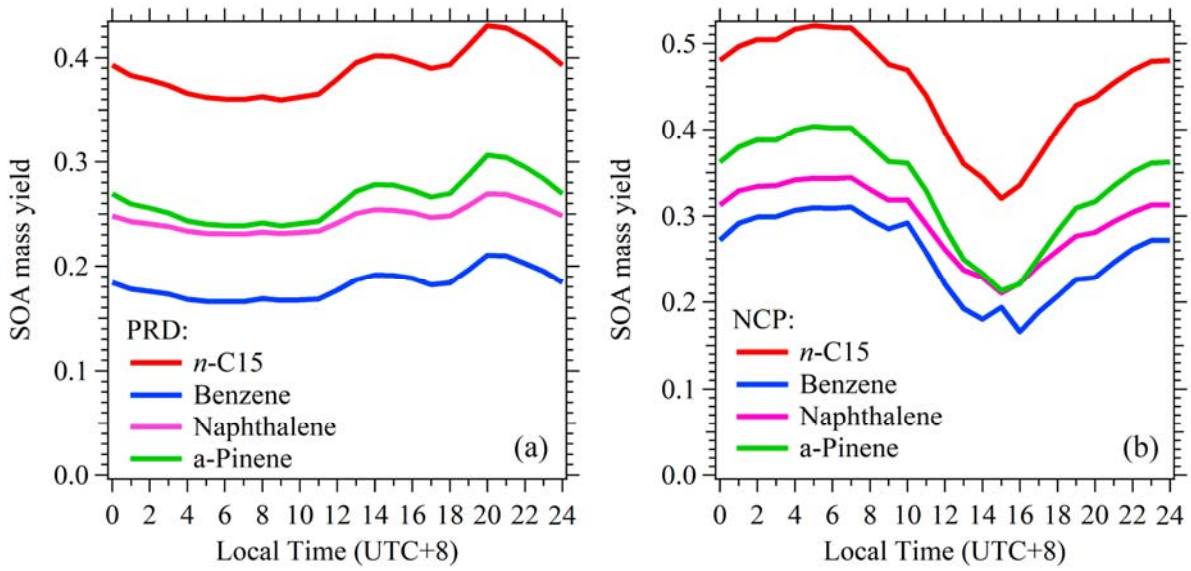

Figure S17. Diurnal variations of SOA yields of *n*-C15 alkane, benzene, naphthalene and *α*-pinene in PRD **(a)** and NCP **(b)**.

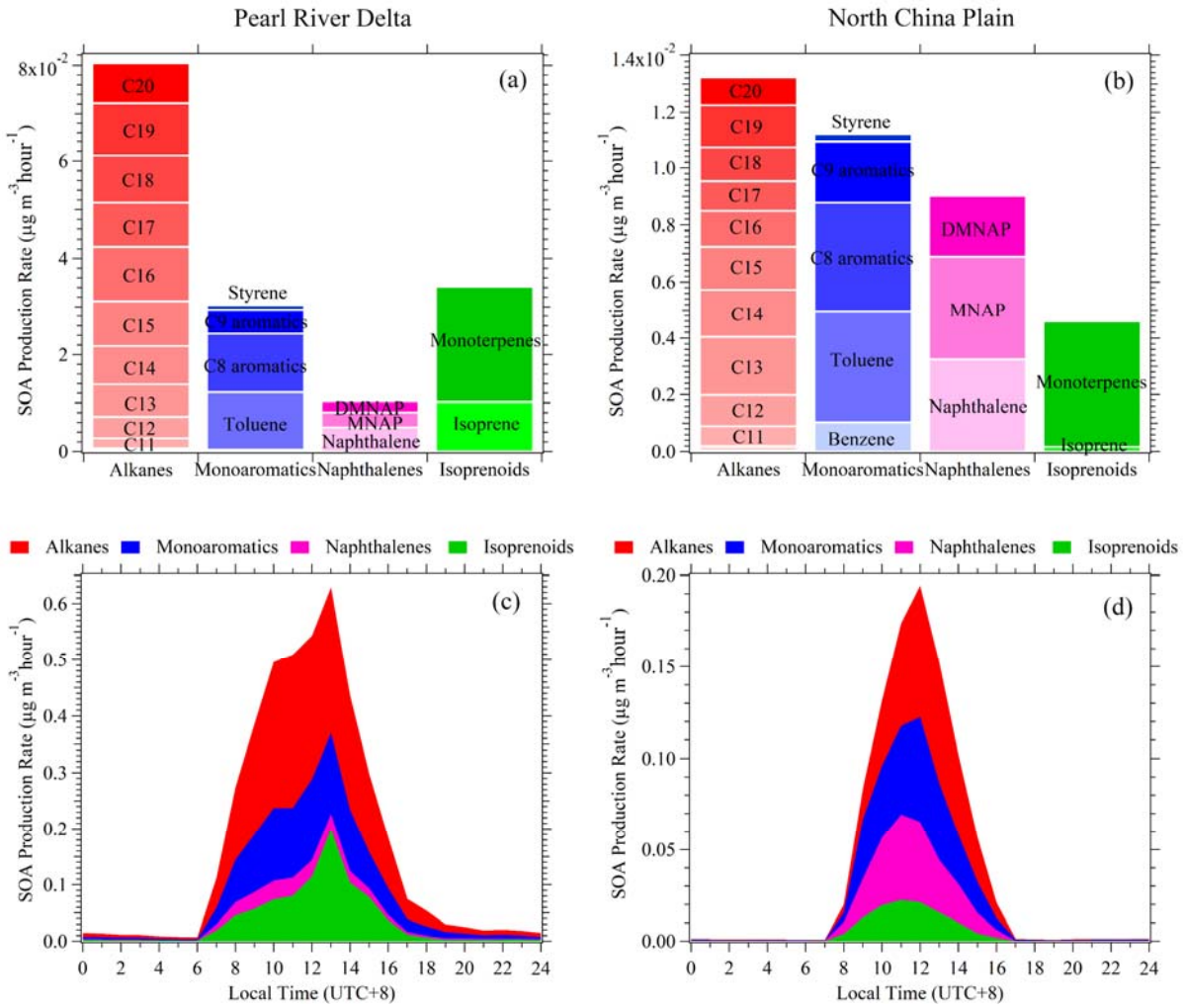

Figure S18. The mean SOA production rates of higher alkanes (C8-C20 alkanes), monoaromatics (benzene, toluene, C8 aromatics, C9 aromatics and styrene), naphthalenes (naphthalene, methylnaphthalenes, dimethylnaphthalenes) and isoprenoids (isoprene and monoterpenes) and their hourly diurnal variations in PRD **(a)** and NCP **(b)**. Diurnal variations of alkanes, monoaromatics, naphthalenes and isoprenoids in PRD **(c)** and NCP **(d)**.

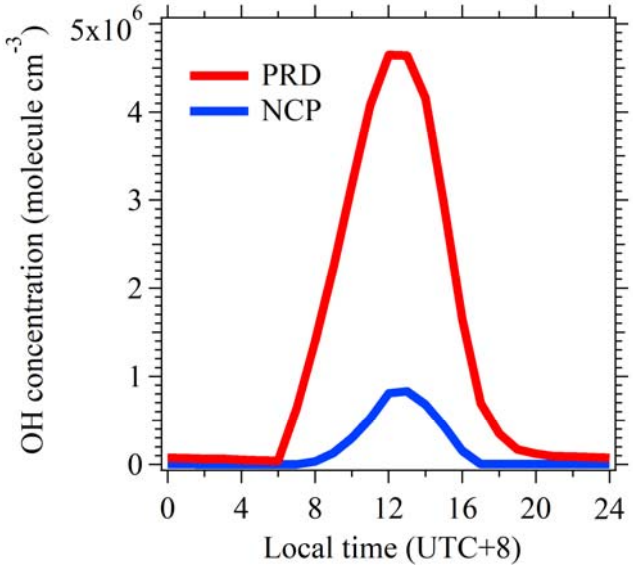

Figure S19. Diurnal variations of OH concentrations in PRD and NCP, respectively. OH concentrations are derived from an observation-constrained box model utilizing MCM v3.3.1 as the chemical mechanisms(Wolfe et al., 2016).

References

Ahlberg, E., Falk, J., Eriksson, A., Holst, T., Brune, W. H., Kristensson, A., Roldin, P., and Svenningsson, B.: Secondary organic aerosol from VOC mixtures in an oxidation flow reactor, Atmospheric Environment, 161, 210-220, 10.1016/j.atmosenv.2017.05.005, 2017.

Atkinson, R.: Kinetics of the gas-phase reactions of OH radicals with alkanes and cycloalkanes, Atmospheric Chemistry and Physics, 3, 2233-2307, 10.5194/acp-3-2233-2003, 2003.

Atkinson, R., and Arey, J.: Atmospheric degradation of volatile organic compounds, Chemical Reviews, 103, 4605-4638, 10.1021/cr0206420, 2003.

Carlton, A. G., Wiedinmyer, C., and Kroll, J. H.: A review of Secondary Organic Aerosol (SOA) formation from isoprene, Atmospheric Chemistry and Physics, 9, 4987-5005, 10.5194/acp-9-4987-2009, 2009.

Chan, A. W. H., Kautzman, K. E., Chhabra, P. S., Surratt, J. D., Chan, M. N., Crounse, J. D., Kuerten, A., Wennberg, P. O., Flagan, R. C., and Seinfeld, J. H.: Secondary organic aerosol formation from photooxidation of naphthalene and alkylnaphthalenes: implications for oxidation of intermediate volatility organic compounds (IVOCs), Atmospheric Chemistry and Physics, 9, 3049-3060, 10.5194/acp-9-3049-2009, 2009.

de Gouw, J. A., Gilman, J. B., Kim, S. W., Lerner, B. M., Isaacman-VanWertz, G., McDonald, B. C., Warneke, C., Kuster, W. C., Lefer, B. L., Griffith, S. M., Dusanter, S., Stevens, P. S., and Stutz, J.: Chemistry of Volatile Organic Compounds in the Los Angeles basin: Nighttime Removal of Alkenes and Determination of Emission Ratios, Journal of Geophysical Research-Atmospheres, 122, 11843-11861, 10.1002/2017jd027459, 2017.

Edney, E. O., Kleindienst, T. E., Jaoui, M., Lewandowski, M., Offenberg, J. H., Wang, W., and Claeys, M.: Formation of 2-methyl tetrols and 2-methylglyceric acid in secondary organic aerosol from laboratory irradiated isoprene/NOX/SO2/air mixtures and their detection in ambient PM2.5 samples collected in the eastern United States, Atmospheric Environment, 39, 5281-5289, https://doi.org/10.1016/j.atmosenv.2005.05.031, 2005.

Hayes, P. L., Ortega, A. M., Cubison, M. J., Froyd, K. D., Zhao, Y., Cliff, S. S., Hu, W. W., Toohey, D. W., Flynn, J. H., Lefer, B. L., Grossberg, N., Alvarez, S., Rappenglueck, B., Taylor, J. W., Allan, J. D., Holloway, J. S., Gilman, J. B., Kuster, W. C., De Gouw, J. A., Massoli, P., Zhang, X., Liu, J., Weber, R. J., Corrigan, A. L., Russell, L. M., Isaacman, G., Worton, D. R., Kreisberg, N. M., Goldstein, A. H., Thalman, R., Waxman, E. M., Volkamer, R., Lin, Y. H., Surratt, J. D., Kleindienst, T. E., Offenberg, J. H., Dusanter, S., Griffith, S., Stevens, P. S., Brioude, J., Angevine, W. M., and Jimenez, J. L.: Organic aerosol composition and sources in Pasadena, California, during the 2010 CalNex campaign, Journal of Geophysical Research-Atmospheres, 118, 9233-9257, 10.1002/jgrd.50530, 2013.

Kleindienst, T. E., Edney, E. O., Lewandowski, M., Offenberg, J. H., and Jaoui, M.: Secondary Organic Carbon and Aerosol Yields from the Irradiations of Isoprene and α-Pinene in the Presence of NOx and SO2, Environmental Science & Technology, 40, 3807-3812, 10.1021/es052446r, 2006.

Lamkaddam, H., Gratien, A., Pangui, E., Cazaunau, M., Picquet-Varrault, B., and Doussin, J.-F.: High-NOx Photooxidation of n-Dodecane: Temperature Dependence of SOA Formation, Environmental Science & Technology, 51, 192-201, 10.1021/acs.est.6b03821, 2017a.

Lamkaddam, H., Gratien, A., Pangui, E., Cazaunau, M., Picquet-Varrault, B., and Doussin, J. F.: High-NOx Photooxidation of n-Dodecane: Temperature Dependence of SOA Formation, Environ Sci Technol, 51, 192-201, 10.1021/acs.est.6b03821, 2017b.

Li, L., Tang, P., Nakao, S., Kacarab, M., and Cocker, D. R., III: Novel Approach for Evaluating Secondary Organic Aerosol from Aromatic Hydrocarbons: Unified Method for Predicting Aerosol Composition and Formation, Environmental Science & Technology, 50, 6249-6256, 10.1021/acs.est.5b05778, 2016.

Lim, Y. B., and Ziemann, P. J.: Effects of Molecular Structure on Aerosol Yields from OH Radical-Initiated Reactions of Linear, Branched, and Cyclic Alkanes in the Presence of NOx, Environmental Science & Technology, 43, 2328-2334, 10.1021/es803389s, 2009.

Loza, C. L., Craven, J. S., Yee, L. D., Coggon, M. M., Schwantes, R. H., Shiraiwa, M., Zhang, X., Schilling, K. A., Ng, N. L., Canagaratna, M. R., Ziemann, P. J., Flagan, R. C., and Seinfeld, J. H.:

Secondary organic aerosol yields of 12-carbon alkanes, Atmospheric Chemistry and Physics, 14, 1423-1439, 10.5194/acp-14-1423-2014, 2014.

Ng, N. L., Kroll, J. H., Chan, A. W. H., Chhabra, P. S., Flagan, R. C., and Seinfeld, J. H.: Secondary organic aerosol formation from m-xylene, toluene, and benzene, Atmospheric Chemistry and Physics, 7, 3909-3922, DOI 10.5194/acp-7-3909-2007, 2007.

Pandis, S. N., Paulson, S. E., Seinfeld, J. H., and Flagan, R. C.: Aerosol formation in the photooxidation of isoprene and β-pinene, Atmospheric Environment. Part A. General Topics, 25, 997-1008, https://doi.org/10.1016/0960-1686(91)90141-S, 1991.

Presto, A. A., Miracolo, M. A., Donahue, N. M., and Robinson, A. L.: Secondary Organic Aerosol Formation from High-NOx Photo-Oxidation of Low Volatility Precursors: n-Alkanes, Environmental Science & Technology, 44, 2029-2034, 10.1021/es903712r, 2010a.

Presto, A. A., Miracolo, M. A., Donahue, N. M., and Robinson, A. L.: Secondary organic aerosol formation from high-NO(x) photo-oxidation of low volatility precursors: n-alkanes, Environ Sci Technol, 44, 2029-2034, 10.1021/es903712r, 2010b.

Tajuelo, M., Rodriguez, D., Teresa Baeza-Romero, M., Diaz-de-Mera, Y., Aranda, A., and Rodriguez, A.: Secondary organic aerosol formation from styrene photolysis and photooxidation with hydroxyl radicals, Chemosphere, 231, 276-286, 10.1016/j.chemosphere.2019.05.136, 2019.

Tkacik, D. S., Presto, A. A., Donahue, N. M., and Robinson, A. L.: Secondary Organic Aerosol Formation from Intermediate-Volatility Organic Compounds: Cyclic, Linear, and Branched Alkanes, Environmental Science & Technology, 46, 8773-8781, 10.1021/es301112c, 2012.

Wolfe, G. M., Marvin, M. R., Roberts, S. J., Travis, K. R., and Liao, J.: The Framework for 0-D Atmospheric Modeling (F0AM) v3.1, Geoscientific Model Development, 9, 3309-3319, 10.5194/gmd-9-3309-2016, 2016.